Adipocyte-secreted exosomal microRNA-34a inhibits M2 macrophage polarization to promote obesity-induced adipose inflammation

Authors: Yong Pan, [1,2] Xiaoyan Hui, [1,2] Ruby Lai chong Hoo, [1,3] Dewei Ye, [4,5] Cyrus Yuk Cheung Chan, [1,2], Tianshi Feng, [1,3] Yu Wang, [1,3] Karen Siu Ling Lam, [1,2] Aimin Xu, [1,2,3*]

Affiliations:

[1] State Key Laboratory of Pharmaceutical Biotechnology, The University of Hong Kong, Hong Kong

[2] Department of Medicine, The University of Hong Kong, Hong Kong

[3] Department of Pharmacy and Pharmacology, The University of Hong Kong, Hong Kong

[4]Joint Laboratory between Guangdong and Hong Kong on Metabolic Diseases, Guangdong Pharmaceutical University, Guangzhou

[5]Guangdong Research Center of Metabolic Diseases of Integrated Western and Chinese Medicine, Guangdong Pharmaceutical University, Guangzhou, China

[*]Correspondence: amxu@hku.hk, L8-40, 21 Sassoon Rd, New Laboratory Block, Pokfulam, Hong Kong

Running title: adipocyte miR-34a controls macrophage polarization

The authors declare that there is no duality of interest associated with this manuscript.

Supplemental Methods

Construction, production and titration of recombinant adeno-associated virus and lentivirus. For generation of adeno-associated virus (AAV) overexpressing *Klf4*, the ORF sequence encoding mouse *Klf4* was subcloned into pAM2AA-eGFP vector via EcoRI and BamHI sites and the empty vector was used as the mock control. The AAV vector, pRep2Cap8 vector and the helper vector were co-transfected into human embryonic kidney (HEK)-293T cells, followed by purification using polyethylene glycol/aqueous two-phase partitioning and titration by real-time quantitative PCR analysis. For the construction of lentivirus delivering small hairpin (sh) RNA targeting *Klf4*, the forward and reverse oligonucleotides were annealed, ligated into the pLKO.1 plasmid via the EcoRI and AgeI restriction sites. To produce lentiviral particles, pLKO.1 shRNA plasmid or scramble shRNA plasmid (as control) with psPAX2 packing plasmid and pMD2.G envelope plasmid were transfected into HEK-293T cells by polyethylenimine-mediated transfection. The titer of the purified virus was determined by real-time quantitative PCR analysis. Sequences of the cloning primers were listed in Table S4. For *in vivo* AAV and lentivirus treatment, 50 μl of 1×10^9 viral particles of AAV or lentivirus was locally injected into epididymal fat pad in mice. Adipose tissues were collected 2 weeks after injection and the efficiency of infection was validated by immunoblot analysis.

For generation of miR-34a sponge lentivirus, the pGMLV-SB1 vector was purchased from Genomeditech (Shanghai, China). The miR-34a or nonsense control miR lentiviral sponge plasmid was constructed by using synthetic oligonucleotide, which contains either four tandem miR-34a binding sites or nonsense sequence as listed in Table S4. MiR-34a sponge lentivirus or control lentivirus was produced by co-transfecting HEK-293T cells with the corresponding lentiviral construct and lentiviral mix (Genomeditech) according to the manufacturer's instruction. For lentivirus encoding miR-34a, pLL3.7 hsa-miR-34a (Addgene) and lentiviral mix were delivered simultaneously to HEK-293T cells. 72 hours

after transfection, lentivirus was collected and concentrated using Polyethylene glycol 6000 (PEG 6000, Sigma) precipitation approach and the titer was determined by real-time quantitative PCR analysis.

Luciferase reporter assay. Plasmid harboring a perfectly complementary binding sequence of miR-34a (psiCHECK2-AS34a) was purchased from Addgene (#37099). The construction of psiCHECK2-*Klf4* (both wild type and mutants) was achieved by digestion of psiCHECK2-AS34a with double restriction enzymes (XhoI and NotI), followed by ligation of sequence encoding the corresponding 3'UTR of the target genes. Sequences of the synthetic oligonucleotides encoding 3'UTR of the target genes and their mutants were listed in Table S2. HEK-293T cells were transfected with one of the above plasmids using Lipofectamine 3000 (Invitrogen) according to the manufacture's instruction. The plasmid expressing constitutively active firefly luciferase (pGL3-Promoter Vector, Promega) was simultaneously delivered to cells for normalization. 48 hours after transfection, cells were lysed and the luciferase activity was assayed with dual-luciferase reporter assay kit (Promega). Data were presented as ratio of renilla luciferase to firefly luciferase activity.

Cell culture and treatments. The murine bone marrow derived cells were isolated from the femur and tibia of C57BL/6J male mice and differentiated into macrophages as described (1). For virus infection, differentiated macrophages were infected with 1 x 10^8 viral particles of adeno-associated virus or lentivirus to overexpress or silence *Klf4*, respectively. Mature adipocytes were isolated from epiWAT of mice using collagenase I digestion as described (2) and cultured in DMEM medium.

Quantitative real-time PCR and immunoblot analysis. Mature adipocytes and SVF were fractionated from adipose tissues using collagenase I digestion and centrifugation as described (2). Total RNA from adipose tissues or its fractions or bone marrow-derived macrophages was extracted with TRIzol reagent (Invitrogen). For mRNA expression analysis, 500 ng of total RNA was used for synthesis of cDNA using PrimeScript RT reagent kit (Takara). For miRNA expression analysis, 150 ng total RNA was reverse-

transcription into cDNA using miRNA-specific primers supplied with TaqMan MicroRNA Reverse Transcription kit. The quantitative real-time PCR was performed using the ABI Prism 7000 instrument (Applied Biosystems). The relative level of gene expressions were calculated by the $2^{-\Delta\Delta CT}$ method, after normalization with the abundance of 18s RNA. Small nucleolar RNA 202 (Sno202) was used as an internal control for comparison of relative changes in miRNA within the same tissue. For comparison of miR-34a in different tissues, the transcribed cDNA was added to each reaction and the Ct values of miR-34a were converted into copy numbers using a standard curve from synthetic lin-4 (3). The sequences of primers used in this study were listed in Supplementary Table 3.

For immunoblot analysis, proteins were extracted from tissues or cells in radioimmunoprecipitation assay (RIPA) buffer (25 mM Tris-HCl pH 7.6, 150 mM NaCl, 5 mM EDTA, 1% NP-40, 1% sodium deoxycholate, 0.1% SDS) containing a complete protease inhibitor cocktail (Roche), resolved by SDS-PAGE, transferred onto polyvinlidene fluoride (PVDF) membranes (Bio-Rad), and then probed with primary antibodies against phospho-AKT (Ser473, #9271), AKT (#9272), Tubulin (#2146) and GAPDH (#3683) from Cell Signaling Technology, or Arginase I (#PA5-29645) and iNOS (#PA5-17106) Thermo Fisher Scientific. Anti-KLF4 (#AF3158) and anti-CD63 (#MAB5417) antibodies were from R&D Systems and Abcam respectively. The protein bands were visualized with enhanced chemiluminescence reagents (GE Healthcare) and quantified by using the NIH ImageJ software.

In Vivo tracking of recruitment of circulating monocytes and proliferation of macrophages in adipose tissues. Peripheral blood of 10-week-old C57BL/6J male mice was collected to heparinized tubes (Fisher) and incubated with 9 volumes of the erythrocyte lysis buffer (0.15 M NH4Cl, 10 mM KHCO3, 0.1 mM EDTA) for 10 min on ice. Afterwards monocytes were isolated from the leukocytes with the EasySep mouse monocyte enrichment kit (Stemcell Tech) and subsequently labeled with the PKH26 labeling kit (Sigma) at a concentration of 2 mM for 1 min. 5×10^6 labeled cells were injected to each recipient mouse via tail vein. 3 days after the injection, SVF of epiWAT was isolated and subjected to flow cytometry

analysis to quantify $PKH26^+$ myeloid cells, $PKH26^+F4/80^+Cd11c^+$ M1 macrophages and $PKH26^+F4/80^+Cd206^+$ M2 macrophages. To measure the proliferation rates of adipose-resident macrophages, mice were injected intraperitoneally with EdU (2 mg/kg/day) in Dulbecco's PBS for 3 days, followed by flow cytometry analysis to quantify proliferating macrophages in SVF of epiWAT.

Flow cytometry analysis. SVF was isolated from epiWAT as described in our previous study (4), resuspended in 1 ml of Live/dead fixable dead cell stain (Molecular Probes) and incubated on ice for 30 min. Afterwards, cells were washed once with FACS buffer (1% BSA in 1xPBS) followed by staining with different antibodies. For flow cytometry analysis of macrophages, 1×10^5 freshly isolated cells were triple stained with F4/80-PE (#123110, Biolegend, 1:100), Cd206-Alexa Fluor 647 (#141708, Biolegend, 1:100), Cd11c-FITC (#117306, Biolegend, 1:100), or their isotype controls (Biolegend) on ice for 30 min in dark. For analysis of eosinophils, 2×10^5 freshly isolated cells were stained with F4/80-FITC (#564227, BD, 1:100), CD11b-PE (#553311, BD, 1:100) and SiglecF-APC (#565183, BD, 1:100). For analysis of ILC2s, 2×10^5 freshly isolated cells were stained with lineage markers: CD25-PE (#558642, BD, 1:100), and IL-33R-AF700 (#MAB10041, R&D, 1:100). After staining, cells were fixed with 2% (w/v) paraformaldehyde and stored at 4°C before analysis with BD LSRFortessa Cell Analyzer (BD Biosciences). Data were analysed using FlowJo software version X.0.7 (Tree Star, Inc.).

Histological and immunochemical analysis. Adipose tissues or liver were fixed in 4 % formalin solution for 48 hours, embedded in paraffin, and sectioned at 5 μm. Deparaffinized and rehydrated sections were stained with haemotoxylin and eosin (Sigma), or with reagents for Oil Red O staining and Sirius red staining, or immunohistological staining of F4/80 (#MAB5580, R&D systems, MN). Tissue sections were visualized with Olympus biological microscope BX41, and images were captured with Olympus DP72 color digital camera.

Purification and characterization of adipocyte-secreted exosomes. Mature adipocytes were isolated from epiWAT of mice using collagenase I digestion as described (2) and cultured in DMEM medium for 48 hours. The exosomes secreted from adipocytes were purified with ultracentrifugation as described previously (5). Briefly, the debris and dead cells in the medium were removed by centrifugation at 1000 g for 5 min and at 10,000 g for 10 min respectively. The medium was filtrated through 0.2 μm filter and subjected to ultracentrifugation at 100,000 g for 2 hours at 4°C. The resulting pellet was suspended in 1× PBS, ultracentrifuged again at 100,000g for 20 min and resuspended in 1× PBS. The characterization of exosomes was confirmed by electron microscopy and immunoblot analysis measuring the expression of the exosome-specific marker CD63 (6). To monitor exosomal trafficking, exosomes were labeled with Dil-C18 fluorescent dye (Sigma-Aldrich) as described (7). After Dil-C18 staining, the exosomes were washed in PBS and collected by ultracentrifugation (100,000 g for 20 min) at 4°C.

Supplementary Tables

Group		Gene name	mirSVR score	PhastCons score
M2 type		*Klf4*	-1.1751	0.5604
		Stat6	-0.3273	0.5417
		PPARg	—	—
		Cebpb	—	—
M1 type		*Stat3*	—	—
		Cebpa	—	—
		Irf5	—	—
	AP1	*c-Fos*	—	—
		c-Jun	—	—
		Atf2-7	—	—
		Jdp	—	—
	NF-κB	*Nfkb1*	—	—
		Nfkb2	—	—
		Rela	—	—
		Relb	—	—
	PU.1	*Sfpi1*	—	—
		Stat1	—	—

Table S1. The predicted scores for the binding of miR-34a to a panel of transcription factors involved in macrophage polarization. The prediction was made using both mirSVR and PhastCons programs.

Variables	Lean (n= 29)	Overweight/obese (n= 24)
Age (years)	44.04 ± 3.16	45.91 ± 4.13
BMI (kg/m^2)	20.50 ± 1.36	26.08 ± 2.41
Total cholesterol (mmol/l)	4.58 ± 0.63	5.17 ± 1.02
Triglycerides (mmol/l)	0.88 ± 0.33	1.19 ± 0.55
Fasting glucose (mmol/l)	4.75 ± 0.43	5.15 ± 0.67
Glucose AUC	13.55 ± 2.75	17.08 ± 4.73
Fasting insulin (μU/ml)	4.63 ± 1.82	7.88 ± 3.58
HOMA-IR	0.99 ± 0.44	1.83 ± 0.95

Table S2. Anthropometric parameters and biochemical indexes. Data are means ± SEM; BMI, body mass index; AUC, area under curve; HOMA-IR, homeostatic model assessment for insulin resistance.

Genes	Forward primers 5’ to 3’	Reversed primers 5’ to 3’
miR-34a flox/flox genotyping	GGTCACAAGACCCTCACCTG	TCACAGCAGACCCTTGATGT
Cre genotyping	AGCGATGGATTTCCGTCTCTGG	AGCTTGCATGATCTCCGGTATTGAA
Klf4 3’-UTR	GGTATCTCTAGAATCCCACGTAGTG GATGTGACCCA	GGTATCTCTAGACGTTCAGATAA AATATTATAGGT
Klf4 mutant 3’-UTR	ATCCCACGTAGTGGATGTGACCCGC GCC GCAGGGAGAGAG	CTCTCTCCCTGCGGCGCGGGTCACAT CCACTACGTGGGAT
Mouse Klf4 cDNA cloning	CCGGAATTCATGAAGCGACTTCCCC CACTTCCC	CGCGGATCCGTGTGGGTCACATCCAC TACGTGGG
Mouse Tnfa	ACGGCATGGATCTCAAAGAC	AGATAGCAAATCGGCTGACG
Mouse Il6	GTCCTTCCTACCCCAATTTCCA	TAACGCACTAGGTTTGCCGA
Mouse Il1b	TGTGAAATGCCACCTTTTGA	GGTCAAAGGTTTGGAAGCAG
Mouse iNos	CCAAGCCCTCACCTACTTCC	CTCTGAGGGCTGACACAAGG
Mouse Mcp1	CCACTCACCTGCTGCTACTCA	TGGTGATCCTCTTGTAGCTCTCC
Mouse Fizz1	GGTCCCAGTGCATATGGATGAGACC ATAG	CACCTCTTCACTCGAGGGACAGTTGG CAGC
Mouse Ym1	TCACAGGTCTGGCAATTCTTCTG	TTTGTCCTTAGGAGGGCTTCCTC
Mouse Arg1	CTCCAAGCCAAAGTCCTTAGAG	AGGAGCTGTCATTAGGGACATC
Mouse Il10	GCTCTTACTGACTGGCATGAG	CGCAGCTCTAGGAGCATGTG
Mouse Col6a1	GATGAGGGTGAAGTGGGAGA	CAGCACGAAGAGGATGTCAA
Mouse Mmp12	ACATTTCGCCTCTCTGCTGATGAC	CAGAAACCTTCAGCCAGAAGAACC
Mouse Tgfb1	CGCCTCTATGAGAAAACC	GTAACGCCAGGAATTGT
Mouse Klf4	GTCAAGTTCCCAGCAAGTCAG	CATCCAGTATCAGACCCCATC
Mouse Il4	GGTCACAGGAGAAGGGACGCC	TGCGAAGCACCTTGGAAGCCC
Mouse Il5	AGGCTTCCTGTCCCTACTCA	CCCCCACGGACAGTTTGATT
Mouse Il13	TGAGCAACATCACACAAGACC	GGCCTTGCGGTTACAGAGG
Mouse 18s	AGTCCCTGCCCTTTGTACACA	CGATCCGAGGGCCTCACTA
Human TNFA	CCCAGGGACCTCTCTCTAATC	ATGGGCTACAGGCTTGTCACT
Human IL6	GCACTGGCAGAAAACAACCT	TCAAACTCCAAAAGACCAGTGA
Human KLF4	CGAACCCACACAGGTGAGAA	TACGGTAGTGCCTGGTCAGTTC
Human 18S	CAATTACAGGGCCTCGAAAG	AAACGGCTACCACATCCAAG

Table S3. Sequences of primers used for genotyping of mice, cloning and real-time PCR analysis.

Name of the construct	Inserted sequence
sh*Klf4*	5’CCGGCATGTTCTAACAGCCTAAATGCTCGAGCATTTAGGCTGTTAGAACATGTTTT TG 3’
Control shRNA	5’CCGGCTCGTAAATCCGACAATCTTGTACGAGCATTTAGGCTGTTTTTGATGCTTGC GC 3’
miR-34a sponge	5’GATCCACAACCAGCTTCTCACTGCCActacaACAACCAGCTTCTCACTGCCActacaAC AACCAGCTTCTCACTGCCActacaACAACCAGCTTCTCACTGCCAG 3’
Control non-sense sponge	5’GATCCTCTACTCTTTCTTCCGGTTGTGActacgTCTACTCTTTCTTCCGGTTGTGActacg TCTACTCTTTCTTCCGGTTGTGActacgTCTACTCTTTCTTCCGGTTGTGAG 3’

Table S4. Sequences inserted in the constructs for siRNA targeting Klf4 and miR-34a sponge.

References

1. Weischenfeldt J, and Porse B. Bone Marrow-Derived Macrophages (BMM): Isolation and Applications. *CSH protocols.* 2008;2008(pdb prot5080.
2. Hui X, Zhang M, Gu P, Li K, Gao Y, Wu D, Wang Y, and Xu A. Adipocyte SIRT1 controls systemic insulin sensitivity by modulating macrophages in adipose tissue. *EMBO reports.* 2017;18(4):645-57.
3. Chen C, Ridzon DA, Broomer AJ, Zhou Z, Lee DH, Nguyen JT, Barbisin M, Xu NL, Mahuvakar VR, Andersen MR, et al. Real-time quantification of microRNAs by stem-loop RT-PCR. *Nucleic acids research.* 2005;33(20):e179.
4. Hui X, Gu P, Zhang J, Nie T, Pan Y, Wu D, Feng T, Zhong C, Wang Y, Lam KS, et al. Adiponectin Enhances Cold-Induced Browning of Subcutaneous Adipose Tissue via Promoting M2 Macrophage Proliferation. *Cell metabolism.* 2015;22(2):279-90.
5. Ying W, Riopel M, Bandyopadhyay G, Dong Y, Birmingham A, Seo JB, Ofrecio JM, Wollam J, Hernandez-Carretero A, Fu W, et al. Adipose Tissue Macrophage-Derived Exosomal miRNAs Can Modulate In Vivo and In Vitro Insulin Sensitivity. *Cell.* 2017;171(2):372-84 e12.
6. Kowal J, Arras G, Colombo M, Jouve M, Morath JP, Primdal-Bengtson B, Dingli F, Loew D, Tkach M, and Thery C. Proteomic comparison defines novel markers to characterize heterogeneous populations of extracellular vesicle subtypes. *Proceedings of the National Academy of Sciences of the United States of America.* 2016;113(8):E968-77.
7. Zhou Y, Xiong M, Niu J, Sun Q, Su W, Zen K, Dai C, and Yang J. Secreted fibroblast-derived miR-34a induces tubular cell apoptosis in fibrotic kidney. *Journal of cell science.* 2014;127(Pt 20):4494-506.

Figure S1

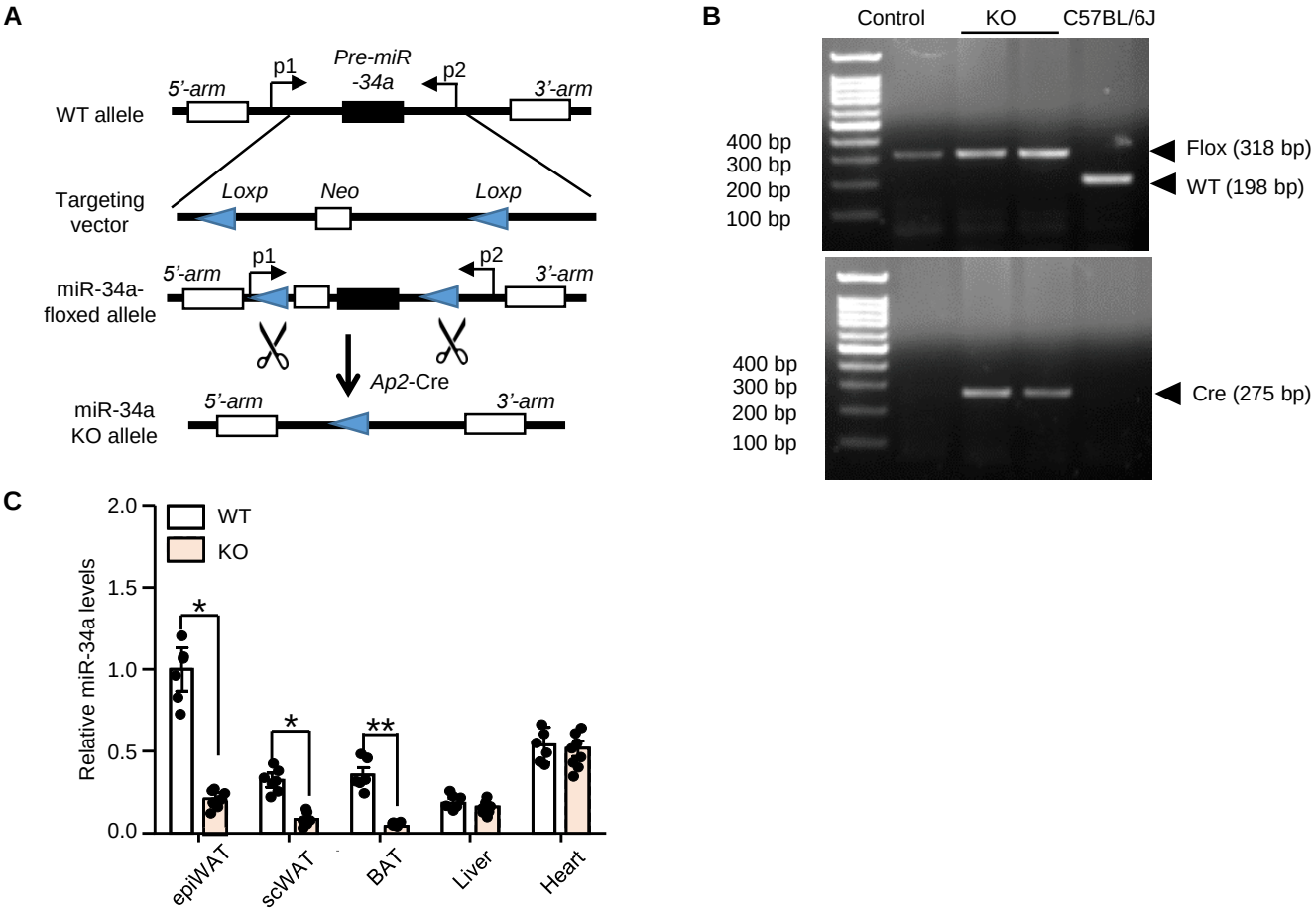

Figure S1. Generation of adipose-selective miR-34a KO mice. (**A**) Schematic diagram showing the strategy for generation of adipose-specific miR-34a KO mice. A targeting vector was designed to insert a *loxP* site upstream of the pre-miR-34a sequence, and a *frt*-flanked neomycin resistance (neo) cassette, followed by a second *loxP* site, downstream of the pre-miR-34a sequence. The primers (p1, p2) spanned the pre-miR-34a region and amplify a band of 198 bp in WT mice, and detected the presence of loxP-Neo region and amplify a band of 318 bp in miR-34a-floxed mice. A set of *ap2*-drived Cre-recombinase (Cre) coding sequence-specific primers amplified a band of 275 bp in Cre+ mice. (**B**) Genotypic PCR analysis showing that the adipose tissue miR-34a WT mouse carrying homozygous miR-34a flox allele, while KO mouse carrying both flox and Cre allele. Lane 1: Offspring from miR-34a WT colony as control; Lane2 and 3: Offspring from miR-34a KO colony; Lane 4: C57BL/6J mouse. (**C**) Real-time PCR analysis showing a markedly decreased expression of miR-34a in several adipose tissues (epiWAT, scWAT, BAT), but not in liver or heart tissues (n = 6-8). Data represent Mean ± SEM. Differences were determined by Student's *t* test (**C**); *P < 0.05, **P < 0.01. MiR-34a abundance was normalized to sno202 level.

Figure S2

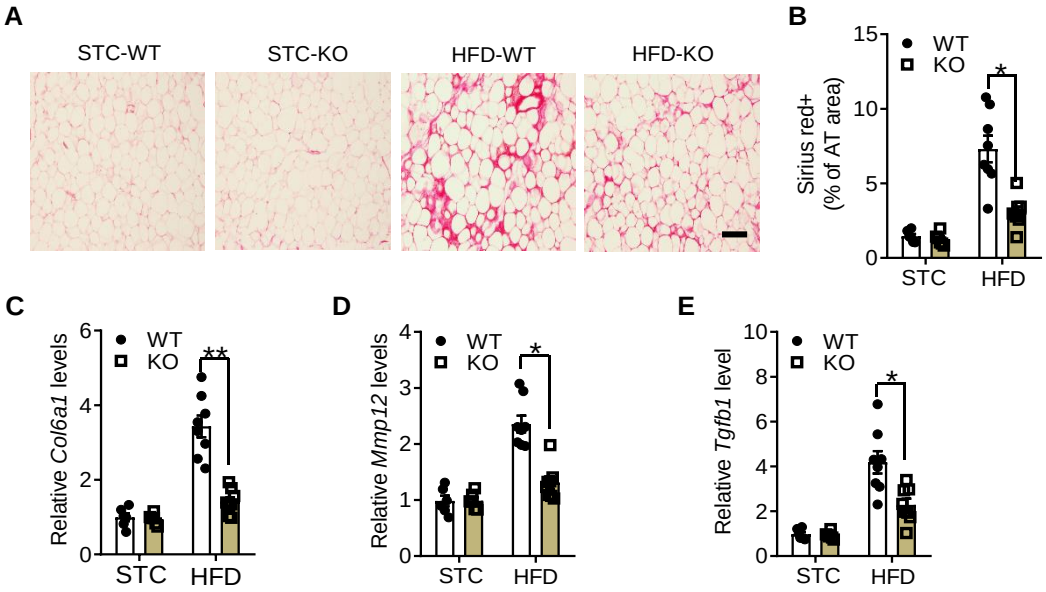

Figure S2. Adipose-specific miR-34a deficiency inhibits dietary obesity-induced adipose fibrosis. 4-week-old male adipose-selective miR-34a KO mice and their WT littermates were fed STC or HFD for 16 weeks. (**A**-**B**) Representative images of Sirius red staining of collagen (**A**), and quantification of Sirius red-positive area (**B**) in epiWAT. Scale bar: 100 μm. (**C**-**E**) Real-time PCR analysis for the mRNA levels of several fibrosis-related genes (*Col6a1, Mmp12, Tgfb1*) in epiWAT (n = 6-8). Data represent mean values ± SEM. Differences between groups were determined by ANOVA (**B**-**E**); *P < 0.05. Gene levels were normalized to *18s* RNA abundance.

Figure S3

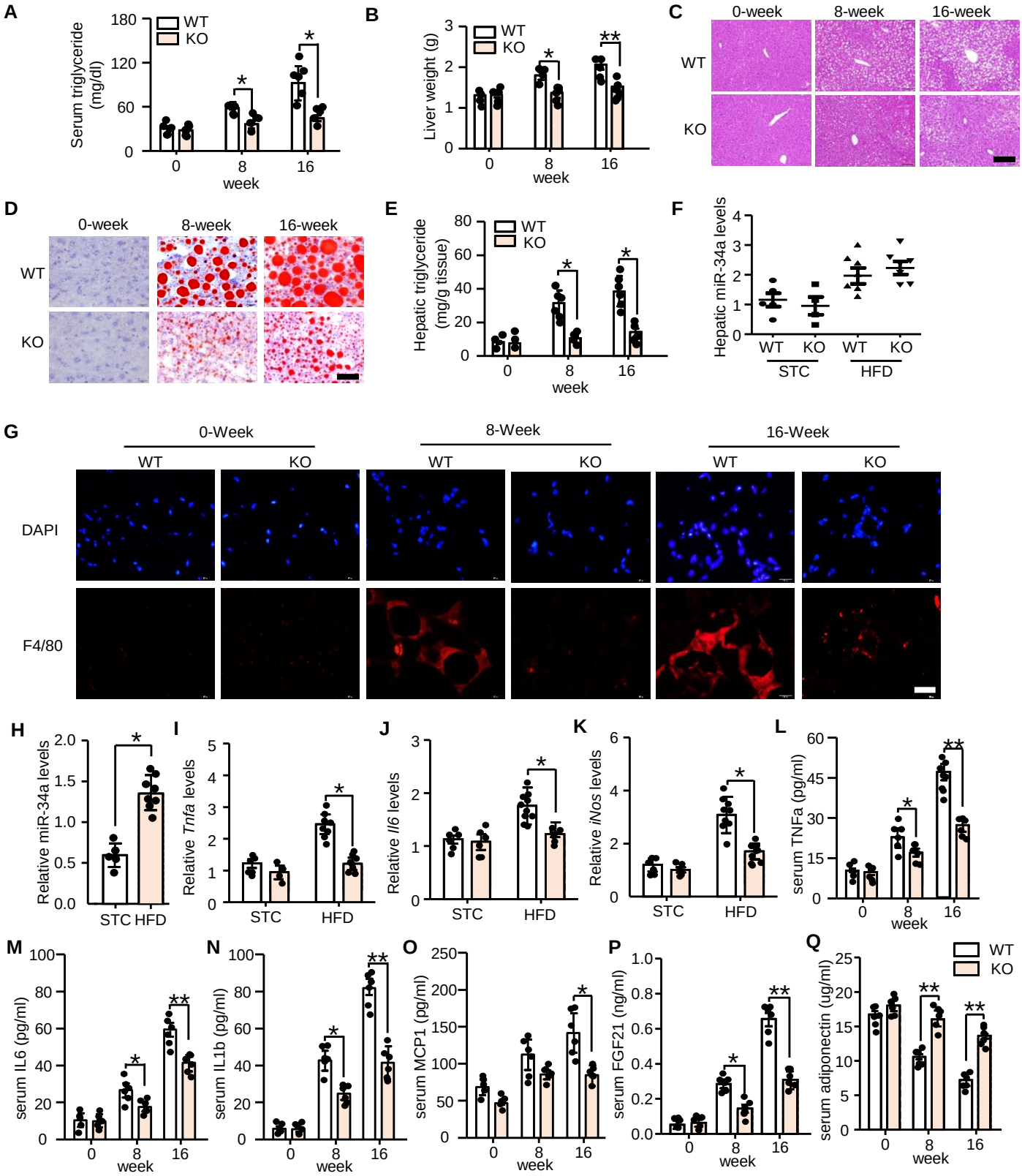

Figure S3. Adipose-specific miR-34a deficiency decreases dietary obesity-induced fatty liver, inflammation in subcutaneous adipose tissue, and systemic inflammation. 4-week-old male adipose-selective miR-34a KO mice and their WT littermates were fed HFD for 0, 8, 16 weeks. Serum triglyceride levels (**A**), liver weight (**B**) and H&E staining (**C**). Oil red O staining for lipid deposition in liver (**D**), and biochemical assay for hepatic triglyceride content (**E**). (**F**) Real-time PCR analysis for the abundance of hepatic miR-34a in the KO mice or WT littermates on STC or HFD for 16 weeks (n = 6). (**G**) Immunoflurescence staining of F4/80 (red color) and DAPI (blue color) positive cells in epiWAT. Scale bar: 40 μm. (**H**) The abundance of miR-34a in the subcutaneous white adipose tissue (scWAT) of mice on STC or HFD for 16 weeks (n = 6-8). **(I-K**) Real-time PCR analysis for the mRNA levels of the M1 markers in scWAT of mice on STC or HFD 16 weeks (n = 6-8). (**L-Q**) ELISA analysis to measure serum levels of TNFa (**L**), IL6 (**M**), IL1b (**N**), MCP1 (**O**), FGF21 (**P**) and adiponectin (**Q**) in mice on HFD for 0, 8 and 16 weeks (n = 6). Data represent mean values ± SEM. Differences between groups were determined by ANOVA (**A-B**, **E**, **I-Q**) or student's test (**H**); *P < 0.05, **P < 0.01. MiR-34a abundance was normalized to sno202 level, and other gene levels were normalized to *18s* RNA abundance.

Figure S4

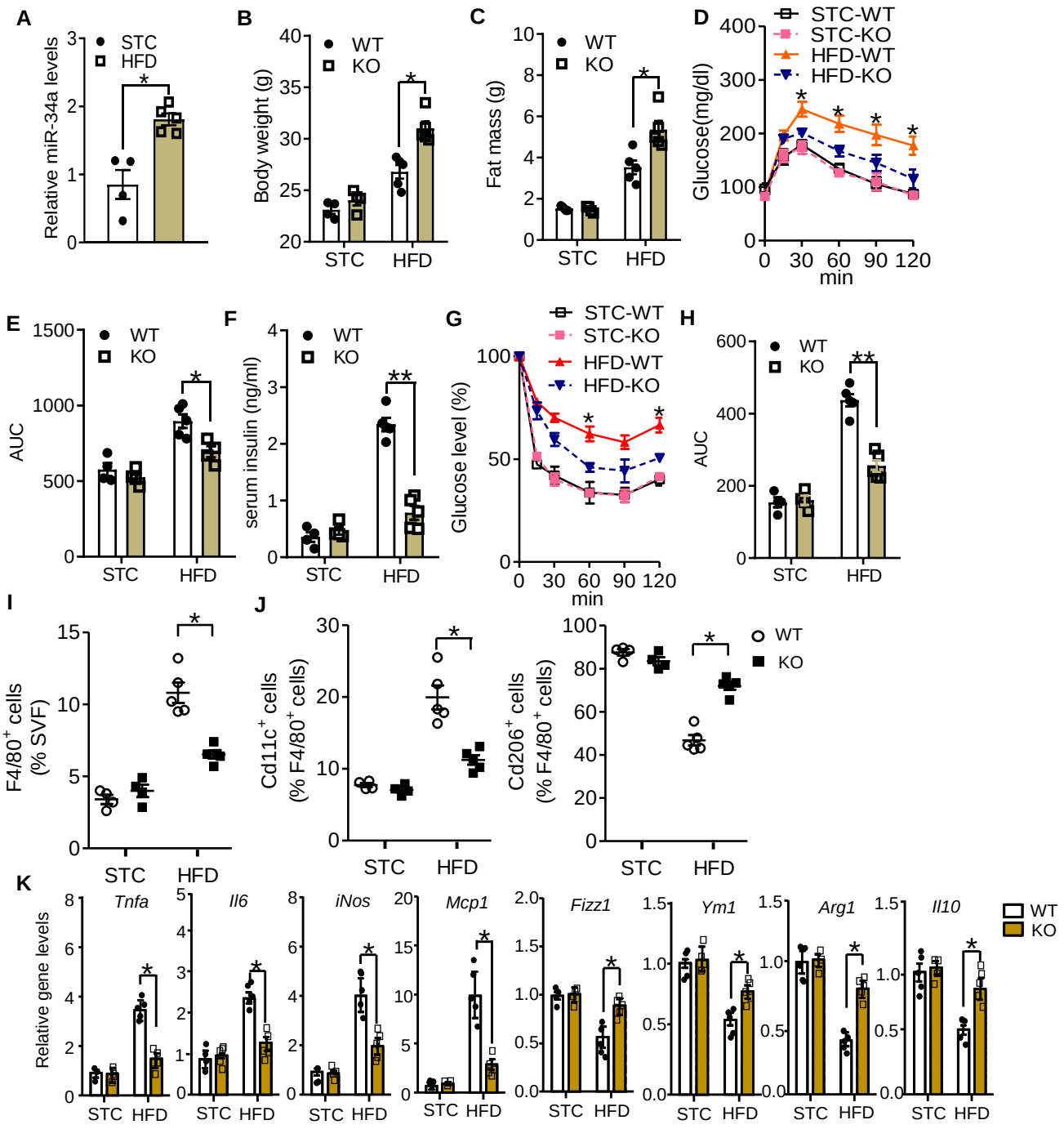

Figure S4. Adipose miR-34a deficiency attenuates glucose intolerance, insulin resistance and adipose inflammation in obese female mice. (**A**) 4-week-old female mice were fed STC or HFD for 12 weeks. Real-time PCR analysis of miR-34a levels in epiWAT (n = 4-5). (**B-J**) 4-week-old female adipose-selective miR-34a KO mice and their WT littermates were fed STC or HFD for 12 weeks. The body weight (**B**) and total fat mass (**C**) were measured immediately after sacrificing the mice (n = 4-5). (**D**) Glucose tolerance test and (**E**) AUC of glucose tolerance test at week 11 after feeding HFD/STC (n = 4-5). (**F**) Serum insulin level, (**G-H**) Insulin tolerance test (**G**) and area under curve (**H**) at week 12 after feeding HFD/STC (n = 4-5). (**I-J**) Flow cytometric quantification for percentage of $F4/80^+$ total macrophages (**I**), $Cd11c^+Cd206^-$ M1 macrophages and $Cd206^+Cd11c^-$ M2 macrophages (**J**) in SVFs of gonadal WAT (n = 4-5). (**K**) Real-time PCR analysis for the mRNA levels of the M1 and M2 markers in gonadal WAT of mice (n = 4-5). Data represent mean values ± SEM. Differences between groups were determined by student's *t* test (**A**) or ANOVA (**B-K**); *P < 0.05, **P < 0.01. MiR-34a abundance was normalized to sno202 level, other gene levels were normalized to *18s* RNA abundance.

Figure S5

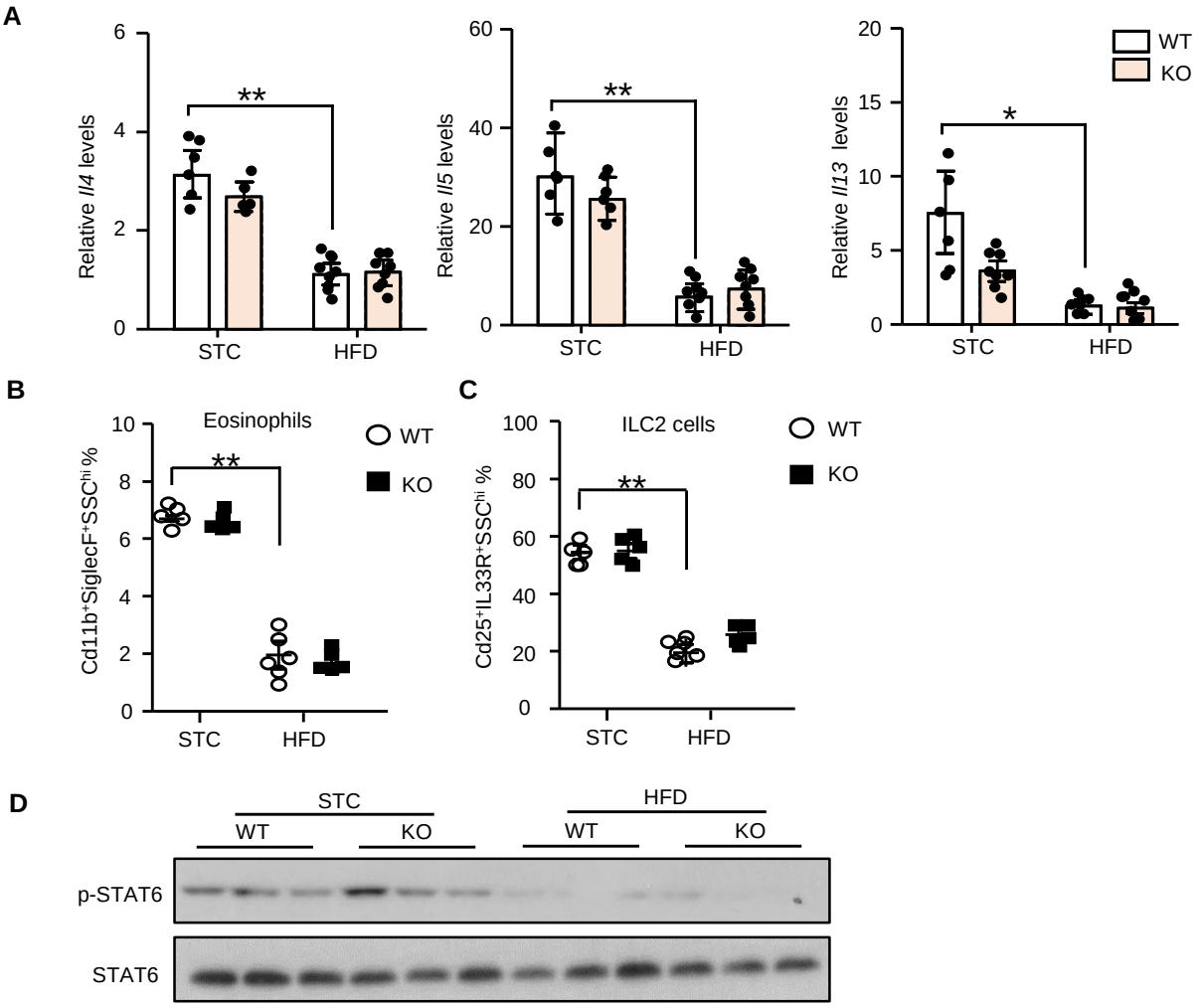

Figure S5. Adipose-selective miR-34a deficiency does not affect the production of several Th2 cytokines and abundance of type-2 immune cells in adipose tissues. Male adipose-selective miR-34a KO mice and their WT littermates were fed with either STC or HFD for 16 weeks. (**A**) The mRNA levels of *Il4*, *Il5* and *Il13* in epiWAT were quantified by real-time PCR (n = 6-8). Quantitative flow cytometry analysis for the percentage of eosinophils (**B**) and ILC2 cell (**C**) in epiWAT (n = 5-6). Eosinophils were identified as $F4/80^{+}Cd11b^{+}$ $SiglecF^{+}SSC^{hi}$ cells, and ILC2s were identified as $Cd25^{+}IL\text{-}33R^{+}SSC^{hi}$ cells respectively. (**D**) Immunoblot analysis for the protein levels of phospho-STAT6 (Tyr641) and total STAT6 in epiWAT. Data represent mean values ± SEM. Differences between groups were determined by ANOVA (**A**-**C**); *P < 0.05, **P < 0.01. Gene levels were normalized to *18s* RNA abundance.

Figure S6

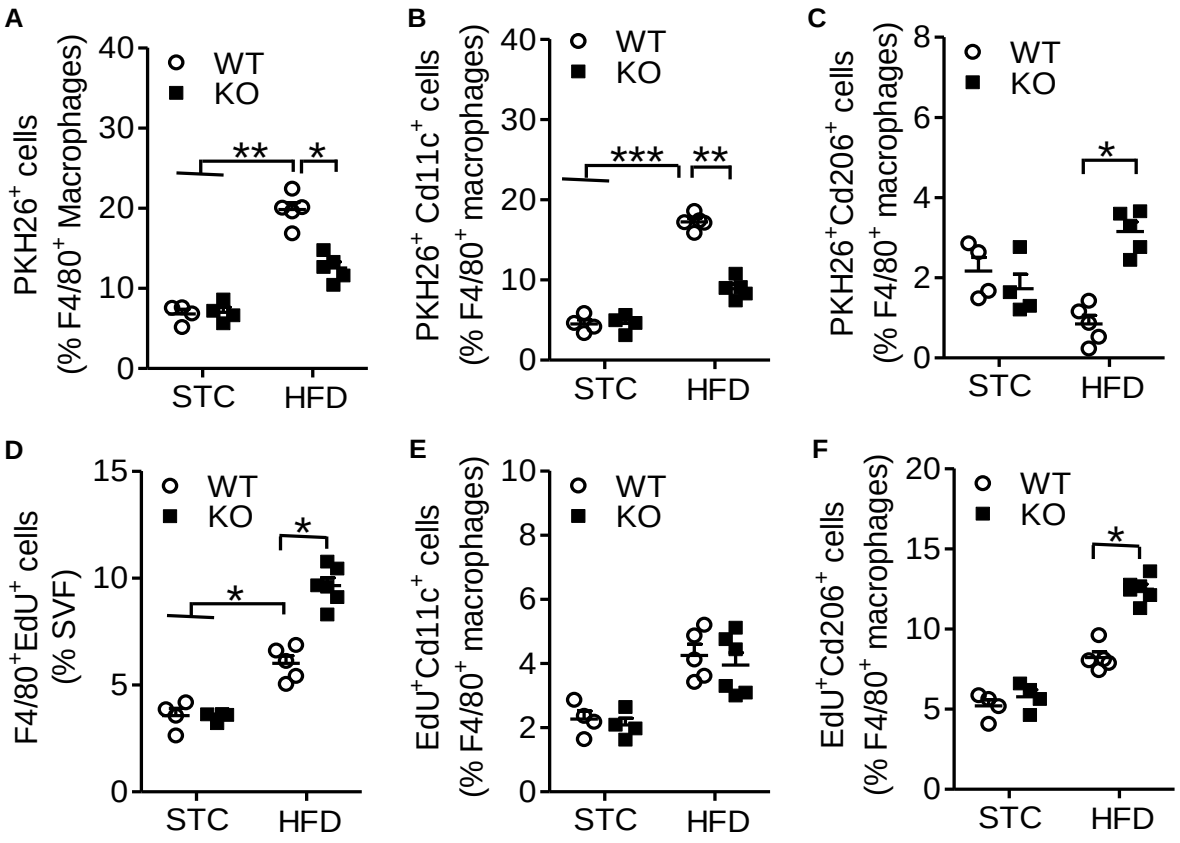

Figure S6. Effects of miR-34a deficiency on recruitment and macrophage conversion of circulating monocytes, and local macrophage proliferation in adipose tissues. (**A**-**C**) 5×10^6 monocytes isolated from peripheral blood of 10-week-old C57BL/6J mice were labeled with PKH26 and injected to adipose-selective miR-34a KO mice and their WT littermates on either STC or HFD for 10 weeks. After three days, mice were sacrificed for collection of epiWAT and isolation of SVF. The percentage of $PKH26^+$ myeloid cells (**A**), $PKH26^+Cd11c^+$ cells (**B**) and $PKH26^+Cd206^+$ cells (**C**) of $F4/80^+$ macrophages in SVF of epiWAT was analyzed by flow cytometry (n = 4-5). (**D**-**F**) Male adipose-selective miR-34a KO mice and their WT littermates on either STC or HFD for 10 weeks were daily injected with EdU (2 mg/kg body weight/day) for three consecutive days. Mice were sacrificed at 7 days after injection for collection of epiWAT. Flow cytometry analysis for the percentage of $F4/80^+EdU^+$ cells (**D**), $F4/80^+Cd11c^+EdU^+$ cells (**E**) and $F4/80^+Cd206^+EdU^+$ cells (**F**) in SVF of epiWAT (n = 4-6). Data represent mean values ± SEM. Differences between groups were determined by ANOVA (**A**-**F**); *P < 0.05, **P < 0.01, ***P < 0.001.

Figure S7

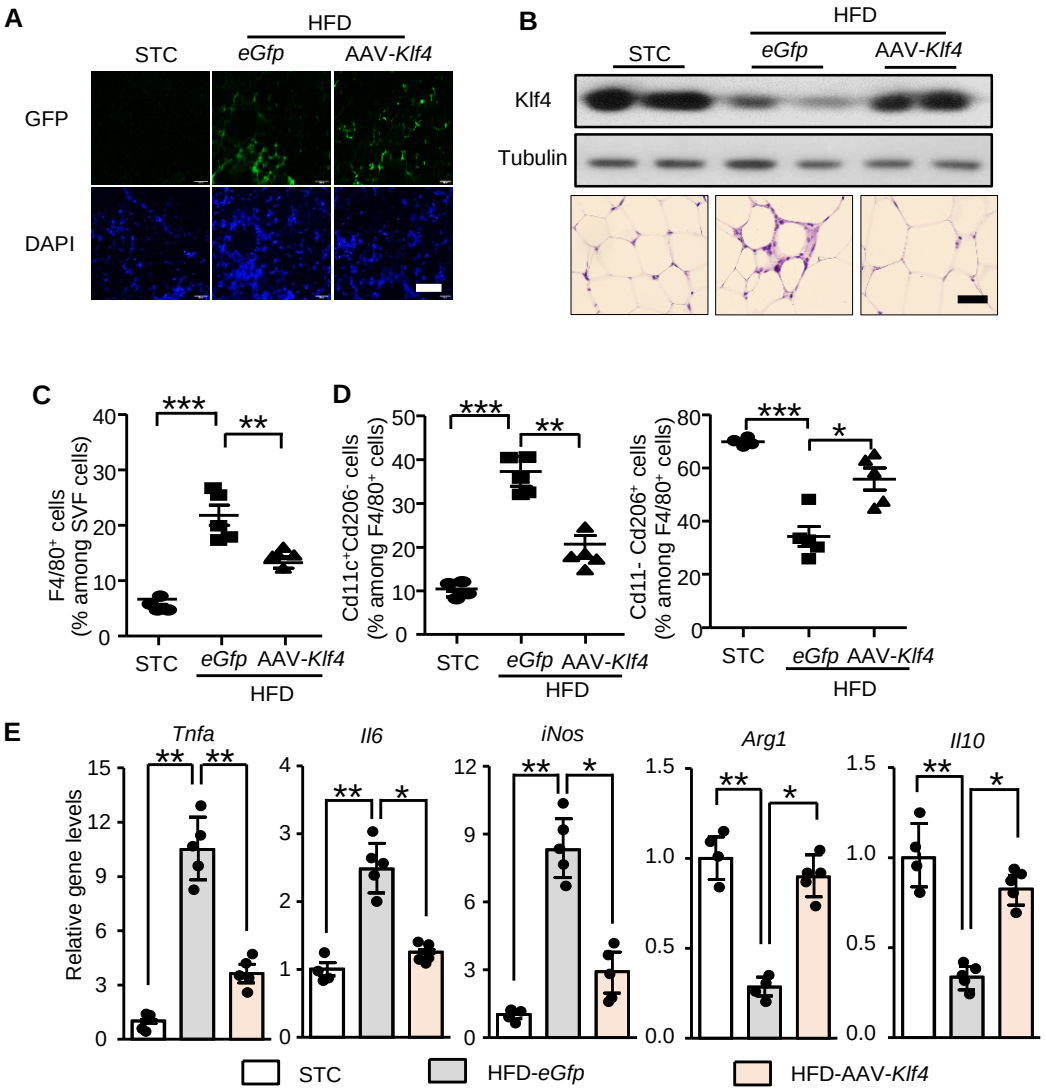

Figure S7. Adipose overexpression of *Klf4* alleviates HFD-induced inflammatory responses in adipose tissues. Male C57BL/6J mice fed with HFD for 14 weeks were locally injected with AAV encoding *Klf4* or *eGfp* in epiWAT (1.2×10^9 viral particles/mouse) for 2 weeks. The mice on STC were used for comparison. (**A**) Representative images of epiWAT showing GFP-positive cells. Scale bar: 200 μm. (**B**) Immunoblot analysis for the abundance of KLF4 protein in SVF (upper panel) and immunohistological staining of F4/80 (lower panel) in epiWAT. (**C**-**D**) Flow cytometric quantification for percentage of $F4/80^+$ total macrophages (**C**), $Cd11c^+Cd206^-$ M1 macrophages and $Cd206^+Cd11c^-$ M2 macrophages (**D**) in SVFs of epiWAT (n = 4-5). (**E**) Real-time PCR analysis for the mRNA abundance of *Tnfa*, *Il6*, *iNos*, *Arg1* and *Il10* in epiWAT (n = 4-5). Data represent mean ± SEM. Differences were determined by ANOVA (**C**-**E**); *P < 0.05, **P < 0.01, ***P < 0.001. Gene levels were normalized to *18s* RNA abundance.

Figure S8

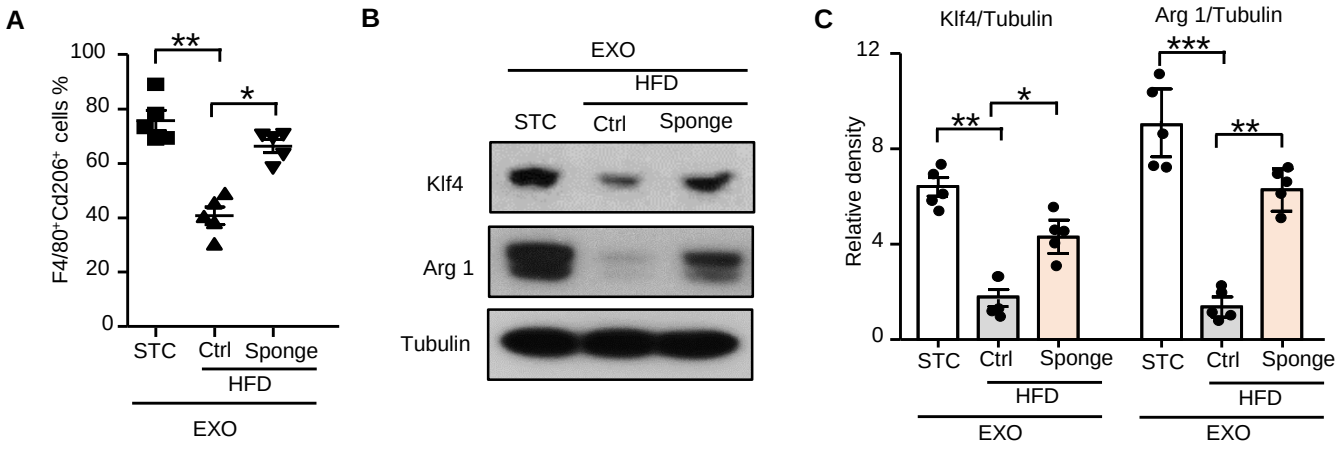

Figure S8. MiR-34a sponge blocks the inhibitory effects of obese adipocyte-derived exosomes on M2 macrophage polarization. Mature adipocytes in epiWAT were isolated from male C57BL/6J mice fed with STC or HFD for 16 weeks, and cultured in 1 ml serum-free DMEM medium for 48 hours. Exosomes were isolated from the conditional medium. BMDMs were infected with lentiviruses encoding miR-34a sponge or control anti-sense (Ctrl) for 24 hours, and then treated with the exosomes in the presence of IL4 for another 24 hours. (**A**) Percentage of M2 macrophages ($F4/80^+Cd206^+$) as determined by flow cytometry (n = 5). Immunoblot analyses of KLF4 and Arg 1 protein levels (**B**), and densitometry analysis of the KLF4/Tubulin and Arg 1/Tubulin ratios (**C**) (n = 5). Data represent Mean ± SEM. Differences were determined by ANOVA (**A**, **C**)*;* *P < 0.05, **P < 0.01, ***P < 0.001.

Figure S9

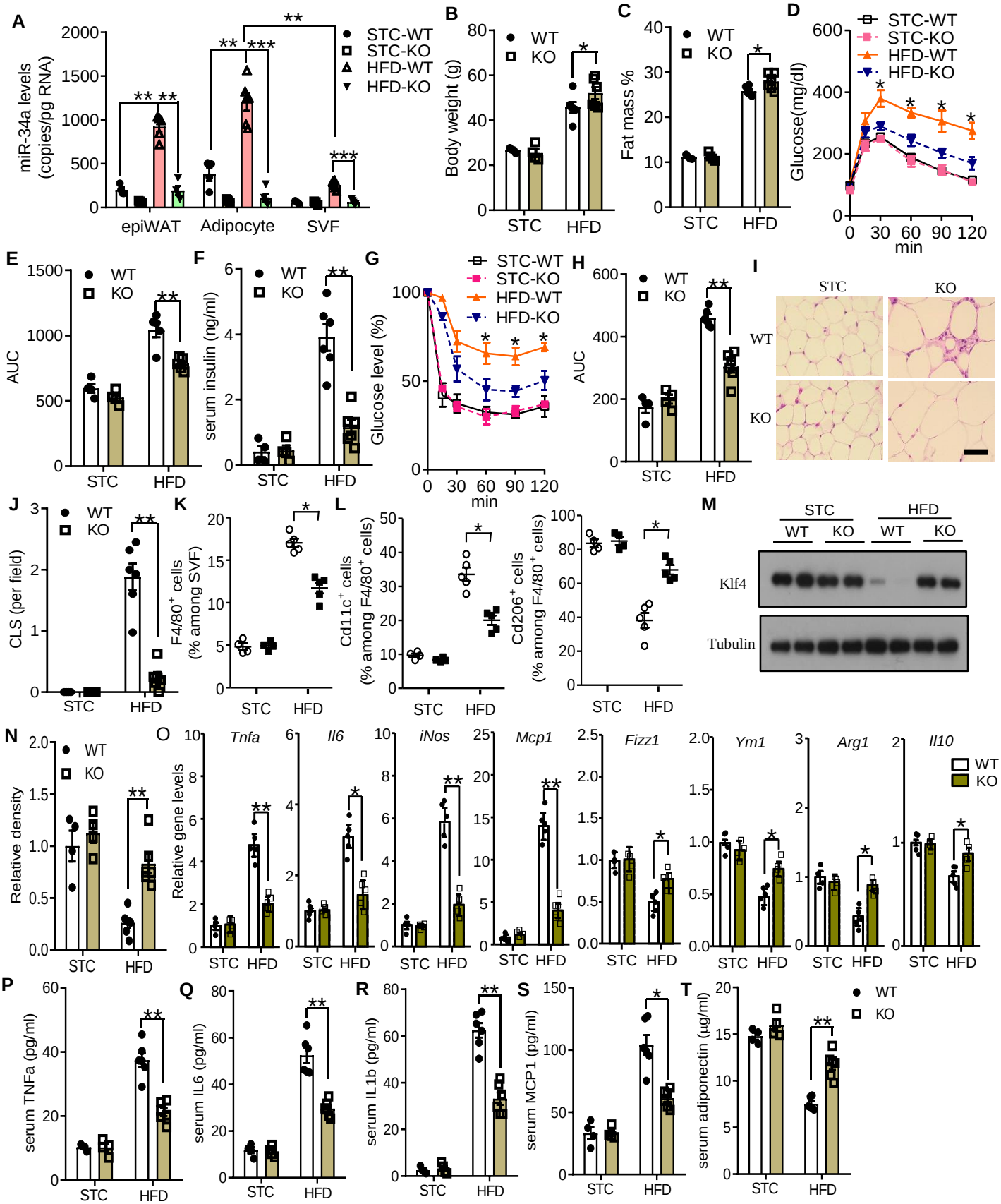

Figure S9. Ablation of miR-34a in adipocytes with the adiponectin promoter-driven Cre protects HFD-induced glucose intolerance, insulin resistance and adipose inflammation in mice. 4-week-old male Adipoq-miR34aKO mice (KO) and their WT miR-34a$^{flox/flox}$ littermates were fed either STC or HFD for 12 weeks. (**A**) Copy numbers of miR-34a in mature adipocytes and stromal vascular fraction (SVF) of epiWAT(n = 4-6). (**B-C**) Body weight (**B**) and percentage of fat mass (**C**) (n = 5). (**D-E**) Glucose tolerance test (**D**) and area under curve (**E**) at week 11 (n = 4-5). (**F**) Fasted serum insulin levels at week 12 (n = 4-5). (**G-H**) Insulin tolerance test (**G**) and area under curve (**H**) at week 12 (n = 4-5). (**I-J**) Representative images of immunohistological staining of F4/80 (**I**) and quantification of crown-like structure (CLS) in epiWAT (**J**) (n = 4-5). (**K-L**) Flow cytometry analysis for percentage of F4/80$^+$ total macrophages (**K**), M1 (Cd11c$^+$Cd206$^-$) and M2 (Cd206$^+$Cd11c$^-$) within the macrophage population in SVF of epiWAT (**L**) (n = 4-5). (**M-N**) Immunoblot analysis for KLF4 protein in in SVF of epiWAT (**M**) and densitometric analysis for their abundance relative to Tubulin (**N**) (n = 4-5). (**O**) Real-time PCR analysis for the mRNA levels of the M1 and M2 markers in SVF of epiWAT. (**P-T**) Serum levels of TNFa (**P**), IL6 (**Q**), IL1b (**R**), MCP1 (**S**), adiponectin (**O**) and FGF21 (**T**) (n = 4-5). Data represent Mean ± SEM. Differences between WT and KO were determined by ANOVA (**A-H**, **J-L**, **N-T**); *P < 0.05, **P < 0.01, ***P < 0.001. Copy numbers of miR-34a were calculated based on a standard curve generated using a synthetic lin-4, mRNA levels were normalized to *18s* RNA abundance.